Journal of Cell Science 107, 2177-2189 (1994)
Printed in Great Britain © The Company of Biologists Limited 1994

Quantification of low density lipoprotein and transferrin endocytic sorting in HEp2 cells using confocal microscopy

Richik N. Ghosh, Dana L. Gelman and Frederick R. Maxfield*

Department of Pathology, Columbia University College of Physicians and Surgeons, Columbia University, 630 West 168th Street, New York, NY 10032, USA

*Author for correspondence

SUMMARY

Numerous experiments on CHO cells have shown that endosomes are composed of separate vesicular and tubulovesicular compartments, such as the sorting endosome, the recycling compartment, and the late endosome. However, Hopkins et al. (*Nature* 346, 335-339, 1990) have reported that endosomes in HEp2 human carcinoma cells form an extensive tubular reticulum. To resolve their observations with previous results from CHO and other cells, we examined the sorting and intracellular transport of endocytosed macromolecules in HEp2 cells, using low density lipoprotein (LDL) and transferrin (Tf) to probe the lysosomally directed and recycling pathways, respectively. Fluorescent LDL and Tf were observed with laser scanning confocal microscopy to visualize simultaneously both probes' sorting and subsequent post-sorting behavior in HEp2 cells. Quantifying the 3-dimensional cellular distributions of fluorescent LDL and Tf, after a variety of pulse-chase schemes, gave the ligands' trafficking rates.

Initially, both ligands appear in the same punctate sorting endosomes, and fingers of Tf start extending from these sorting endosomes. Tf rapidly leaves dual-labeled sorting endosomes ($t_{\frac{1}{2}}$ ~2.5 minutes) and enters a post-sorting recycling compartment from which it is recycled out of the cell ($t_{\frac{1}{2}}$ ~7 minutes). We present both morphological and kinetic data supporting the existence of these two separate compartments along the recycling pathway in HEp2 cells. LDL remains in punctate sorting endosomes that eventually lose the ability to receive newly endocytosed LDL, and mature into late endosomes. The trafficking and sorting of Tf and LDL in HEp2 cells follow the same general scheme as in CHO cells, indicating that the tubular endosomes previously seen may be the tubular parts of the sorting endosomes and recycling compartments in these cells. We propose that the endosomes in the recycling pathway of HEp2 cells, as in CHO cells, are composed of short-lived sorting endosomes, accessible to both Tf and LDL, and long-lived post-sorting recycling compartments, which contain Tf and recycling receptors but not LDL.

Key words: endocytosis, endosome, sorting, HEp2 cell, LDL, low density lipoprotein, transferrin

INTRODUCTION

Various macromolecules that are vital for a cell's proper functioning enter by receptor-mediated endocytosis (Goldstein et al., 1985; van Deurs et al., 1989; McGraw and Maxfield, 1991). In this process, ligands to be internalized bind to their specific receptors on the plasma membrane and cluster in coated pits, which then pinch off into the cell as coated vesicles that deliver their contents to early endosomes. Internalized macromolecules in the early endosomes are sorted into one of two intracellular trafficking routes: (i) the lysosomally directed pathway, by which ligands such as low density lipoprotein (LDL) and α_2-macroglobulin end up in lysosomes via late endosomes (Goldstein et al., 1985; Brown and Goldstein, 1986; van Deurs et al., 1989; McGraw and Maxfield, 1991); and (ii) the recycling pathway, by which recycling proteins such as transferrin (Tf) and the LDL receptor (LDL-R) are recycled back to the plasma membrane (van Deurs et al., 1989; Harford et al., 1991; McGraw and Maxfield, 1991).

The various endosomes involved in the sorting and trafficking of endocytosed molecules are generally considered to be distinct, separate compartments, each with a different pH (McGraw and Maxfield, 1991). However, Hopkins et al. (1990) reported the existence of Tf-containing endosomes that appeared as an extensive tubular reticulum in HEp2 human carcinoma cells, and they proposed movement along the tubular reticulum as a basis for sorting. Tooze and Hollinshead also saw tubular endosomes in HEp2 cells, and confirmed that these tubules were early endosomes that were filled with a fluid-phase label in ~30 minutes (Tooze and Hollinshead, 1991). In contrast, van Deurs et al. (1993) found that endosomes in HEp2 cells were mainly punctate, spherical structures. These observations raised questions as to how Tf is trafficked and sorted in HEp2 cells, and how environments with different pH values might be maintained along a tubular network, if it existed (Warren, 1990).

Extensive work has been done to characterize the recycling and lysosomally directed pathways in Chinese hamster ovary

(CHO) cells. Endocytosed macromolecules are delivered to an acidic (pH ~6) sorting endosome within 2 minutes, where the uncoupling of ligands from their receptors and sorting for proper delivery to the next cellular destination occur (Mellman et al., 1986; Yamashiro and Maxfield, 1987; Sipe and Murphy, 1987; Cain et al., 1989; Presley et al., 1993). Sorting endosomes in CHO cells, which contain newly endocytosed ligands such as LDL, α_2-macroglobulin and Tf, are punctate peripheral compartments with short tubular extensions (Yamashiro et al., 1984). Sorting occurs as an iterative fractionation of membrane components from volume (Dunn et al., 1989). Membrane-associated components in sorting endosomes such as Tf and lipids are then transported to a recycling compartment, presumably by small carrier vesicles (Dunn et al., 1989; Mayor et al., 1993). The recycling compartment in CHO cells is a large, long-lived, condensed tubular structure near the cell's pericentriolar region. It is a distinct compartment from sorting endosomes, is less acidic, and contains sorted recycling material such as Tf, LDL receptors and lipids from the sorting endosome (Yamashiro et al., 1984; Mayor et al., 1993; McGraw et al., 1993). The compartments that contain molecules of the recycling pathway, such as Tf, are often classified as early endosomes (Schmid et al., 1988). Work on CHO cells has shown that the early endosome compartment is composed of two separate and distinct organelles, the sorting endosomes and the recycling compartment.

Pulse-chase experiments with fluorescently labeled LDL or α_2-macroglobulin in CHO cells showed that lysosomally targeted ligands, which are released from their receptors by acidic pH, accumulated in the bulk volume of sorting endosomes, which eventually stopped receiving freshly endocytosed material and matured into late endosomes (Salzman and Maxfield, 1989; Dunn and Maxfield, 1992). Thus, the delivery of lysosomally directed material to late endosomes occurs by a process in which the short-lived sorting endosomes form and then mature into late endosomes. Delivery of material to late endosomes by maturation was also found in other cell types (Murphy, 1991; Stoorvogel et al., 1991; van Deurs et al., 1993).

In this study, our goal was to determine whether the model describing sorting in CHO cells applies to HEp2 cells, or if sorting occurs by a novel tubulo-reticular mechanism. We used Tf as a probe of the recycling pathway and LDL as a probe of the lysosomally directed pathway, and examined where Tf and LDL were in HEp2 cells after a variety of pulse-chase schemes. We used confocal microscopy to simultaneously visualize and quantify the fluorescent Tf and LDL distributions in the entire cell in three dimensions rather than in a single focal plane. Quantifying these images yielded the chronology, itinerary and rate constants for entering and leaving various cellular compartments. We found that HEp2 cells follow a similar endocytic trafficking scheme to CHO cells, where LDL and Tf first enter tubulo-vesicular sorting endosomes and then the Tf is sorted from the LDL and appears in separate recycling compartments, before exiting the cell. LDL remains behind in sorting endosomes, which eventually lose the ability to receive newly endocytosed LDL, and mature into late endosomes.

MATERIALS AND METHODS

Cell culture

HEp2 cells were grown in bicarbonate-buffered Dulbecco's modified Eagle's medium (DMEM) (Gibco Laboratories, Grand Island, NY) supplemented with 5% fetal bovine serum (Gibco), 100 units/ml penicillin and 100 μg/ml streptomycin (Gibco) at 37°C in a 5% CO_2 humidified air atmosphere. 48-72 hours before an experiment, cells were plated in either 6-well plastic dishes for ^{125}I-transferrin experiments or, for optical microscope experiments, in 35 mm diameter plastic tissue culture dishes whose bottoms have been replaced with polylysine-coated no.1 glass coverslips (Salzman and Maxfield, 1988). One day before experiments, the medium was replaced with a similar medium but now containing 5% lipoprotein-deficient serum and 4 μM deferoxamine mesylate (Sigma Chemical Co. St Louis, MO) to stimulate increased expressions of the cells' LDL and Tf receptors (Goldstein et al., 1983; Mattia et al., 1984). Cells whose LDL and Tf receptors had not been upregulated by lipid and iron deprivation, showed similar but dimmer LDL and Tf labeling to those cells in which the receptors had been upregulated. This indicates that lipid and iron deprivation is not altering the endosomal morphologies that we study.

Fluorescent labels

Fluorescein-labeled transferrin (FITC-Tf) was made by first iron-loading human transferrin (Sigma), purifying it by Sephacryl S-300 (Pharmacia LKB, Uppsala, Sweden) gel-filtration chromatography, and then conjugating it to fluorescein isothiocyanate, all as previously described (Yamashiro et al., 1984). diI-LDL and diO-LDL (LDL conjugated to 3,3′-dioctadecylindocarbocyanine (diI) and 3,3′-dioctadecyloxacarbocyanine (diO), respectively) were prepared as previously described (Pitas et al., 1981; Dunn and Maxfield, 1992).

Fluorescent labeling of cells

All labeling was done in air on a 37°C tray. Prior to any fluorescent labeling, the cells were rinsed once and then incubated for 5 minutes with dye-free labeling medium (F-12 medium without bicarbonate, buffered with 20 mM HEPES to pH 7.4, and containing 100 units/ml penicillin, 100 μg/ml streptomycin and 2 mg/ml ovalbumin; Sigma). To study LDL and transferrin sorting, the cells were then incubated for 2 minutes with 20 μg/ml FITC-Tf and 20 μg/ml diI-LDL in labeling medium for 2 minutes. To remove cell surface transferrin, cells were soaked for 2 minutes at 37°C in a pH 4.6 citrate buffer (containing 25.5 mM citric acid, 24.5 mM sodium citrate, 280 mM sucrose and 0.01 mM deferoxamine mesylate), followed by two rinses in a pH 7.4 chase medium (McCoy's 5A medium without bicarbonate, buffered with 20 mM HEPES to pH 7.4, and containing 100 units/ml penicillin, 100 μg/ml streptomycin, 50 μM deferoxamine mesylate and 100 μg/ml of unlabeled transferrin). This impermeant mild acid wash/neutral rinse procedure is a modification of the protocol of Salzman and Maxfield (1988), and it removed ~95% of the cell surface transferrin. The lack of effects of mild acid washing on cell viability and endocytic kinetics have been validated in earlier publications (Presley et al., 1993; McGraw and Maxfield, 1990; Dunn et al., 1989; Salzman and Maxfield, 1988). The procedure did not affect the endocytic machinery of HEp2 cells, as the cells remained viable following the acid wash and rinses, and could still undergo endocytosis at similar rates to cells that were not mild-acid-washed. In addition the rates for Tf to leave the sorting endosome and the whole cell were similar in cells that had or had not been mild-acid-washed, as can be seen in the similar rates obtained from the Tf pulse-chase experiments compared to the Tf accumulation experiments described later in this paper. The cells were then chased for different lengths of time in the chase medium, fixed and prepared for microscopy. Unless otherwise noted, fixation for all experiments was in 2.5% paraformaldehyde freshly diluted in medium 1 (150 mM NaCl, 20 mM HEPES, pH 7.4, 1 mM $CaCl_2$, 5 mM KCl, 1 mM $MgCl_2$) for 2 minutes. After four rinses in medium 1, SlowFade reagent (1,4-diazabicyclo-2,2,2-octane (DABCO) in glycerol/phosphate buffered saline; Molecular Probes) was applied. This was removed and fresh SlowFade reagent was reapplied. The SlowFade

reagent reduced photobleaching of the FITC-Tf, and did not affect diI-LDL staining. This gentle fixation procedure did not noticeably alter the morphologies of the FITC-Tf- and diI-LDL-containing endosomes. Similar structures were seen in fixed cells as in live cells, and while we could not carry out detailed kinetic analysis in live cells, all of the sorting and recycling behavior was qualitatively the same as in the gently fixed cells.

Transferrin uptake in HEp2 cells was studied by labeling the cells for different lengths of time with 5 μg/ml FITC-Tf in labeling medium. During the final 4 minutes of transferrin labeling, 20 μg/ml diI-LDL in labeling medium was added, followed by fixation. If the FITC-Tf labeling time was less than 4 minutes, the diI-LDL was first applied and then the FITC-Tf was added at the appropriate time, giving a total diI-LDL labeling time of 4 minutes.

diI-LDL uptake in cells was studied by incubating the cells with 20 μg/ml diI-LDL in labeling medium for different lengths of time. All the images could not be viewed at the same gain of the confocal microscope's photomultiplier tube, as the diI-LDL intensities at later time points saturated the detector's 8 bit dynamic range. We recorded the 8-17 minute samples at a lower gain setting than the 1-5 minute samples. To compare images taken at the two gain settings, a calibration image was taken of the same field of view of the 8 minute sample at each gain. Background was subtracted from each calibration image, and then ratios of the maximum power (integrated intensity) of the same diI-LDL spots from each image were measured. The mean diI-LDL powers (integrated intensities) per spot in the 8-17 minute samples were multiplied by the mean ratio, so they could be plotted on the same scale with the mean diI-LDL powers per spot of the 1-5 minute samples.

FITC-Tf exit from cells was studied by first labeling the cells with 5 μg/ml FITC-Tf in labeling medium for 1 hour, followed by the mild acid/neutral wash procedure, and then chasing for different lengths of time with the chase medium. Fusion accessibility and maturation of sorting endosomes were studied by labeling the cells with a 3 minute pulse of 20 μg/ml diO-LDL in labeling medium, followed by chases for different lengths of time with labeling medium (containing no dyes), and then a 2 minute pulse of 2 μg/ml diI-LDL in labeling medium, a 2 minute additional chase and fixation.

Confocal microscopy

Fluorescence images of cells were obtained with a Bio-Rad MRC 600 laser scanning confocal microscope (Bio-Rad Microscience, Cambridge, MA) on an inverted Zeiss Axiovert microscope (Zeiss, Oberkochen, Germany) using a 63× (NA 1.4) Zeiss Plan-apo infinity corrected objective. The illumination sources were the 488 nm and 514 nm lines from a 25 mW argon laser. FITC-Tf was visualized with a 488 nm band-pass excitation filter, a 510 nm dichroic mirror and a 515 nm long-pass emission filter. diI-LDL was visualized with a 514 nm band-pass excitation filter, a 540 nm dichroic mirror and a 550 nm long-pass emission filter. The confocal microscope had two photomultiplier tubes enabling detection of two fluorophores simultaneously. To simultaneously visualize FITC-Tf with diI-LDL, a 514 nm excitation filter was used. Fluorescence emissions were selected with a 527 nm dichroic mirror and divided between the two photomultiplier tubes by means of a 565 nm dichroic mirror and a 600 nm long-pass emission filter for diI-LDL, and a 525-555 nm band-pass filter for fluorescein.

The confocal microscope was calibrated using 300 nm fluorescent beads (Wells et al., 1990) in order to determine the dependence of the image slice vertical thickness on the aperture size. Five fields of cells were recorded for each dish. Each field of cells was sectioned 3-dimensionally by recording images from a series of focal planes. Moving from one focal plane to the next was achieved by a stepper motor attached to the fine focus control of the microscope, and the step sizes (in the range between 0.5 μm to 1.25 μm) were chosen with regard to the aperture size being used, so that there would be some overlap between adjacent vertical sections. Enough vertical sections were taken so that the tops and bottoms of all the cells in each field would be recorded. A 10% neutral density filter in the excitation path was used to reduce photobleaching. Each image collected was the average of four scans at the confocal microscope's normal scan rate. Photobleaching was not a problem as diI-LDL's photobleaching was negligible under these conditions and the SlowFade reagent prevented FITC-Tf photobleaching. During each imaging session calibration images were taken of: (i) a microscope slide containing medium 1, in order to measure background levels; (ii) a slide containing diI dissolved in DMSO; and (iii) (if needed) a slide containing either FITC-Tf, or diO dissolved in DMSO.

Image processing and quantification

Image processing and quantification was done on a Gould-Vicom IP9000 image processor (Vicom Visual Computing, Fremont, CA) run by a micro-VAX-II minicomputer (Digital Equipment Corporation, Maynard, MA). The background image was first subtracted from each image in a 3-dimensional stack. Then a 2-dimensional projection was made of the 3-dimensional stack of images, where each pixel's intensity of the next vertical slice was compared with the pixel intensities of the projection thus far, and the maximum intensity was retained. For dual-labeled samples, before the projection was made, each image in a stack was corrected for leakage of emission light from one fluorophore through the barrier filters into the other fluorophore's detector. This was done by measuring the fraction of leakage of one fluorophore into the other fluorophore's detector on a pixel-by-pixel basis, using the calibration images of diI and FITC-Tf, and then subtracting that fraction of the original image from the image receiving the leaked light. With the filter sets used, 15±1% of the diI fluorescence per punctate endosome leaked into the green detector (mean ± s.e.m.), and 7±1% of the FITC and 19±2% of the diO fluorescence per punctate endosome leaked into the red detector. To ensure that this excitation light leakage-correction procedure worked every time, we labeled control dishes of cells with one fluorophore only, recorded their images in the dual imaging mode, and then tested this correction procedure on them.

Image stacks were also viewed on a Tektronix SGS625 color stereo monitor (Tektronix Inc., Beaverton, OR) to localize the different probes in three dimensions with each other. There was very little overlap in the projection image of fluorescent structures from different vertical slices, as they typically followed the contours of the cell's surface.

Prior to quantifying the amount of fluorescent probes present, the remaining background in the projection image was removed by subtracting the median pixel intensity determined from a region in the image lacking cells. To identify the amount of FITC-Tf in diI-LDL spots, the diI-LDL image was used as a mask to select the regions in the FITC-Tf image where FITC-Tf was colocalized with diI-LDL. The fluorescence power in the selected regions of the FITC-Tf images was then normalized to the number of diI-LDL spots, giving the average FITC-Tf fluorescence power per diI-LDL spot. Fig. 3g illustrates how our image processing selected FITC-Tf in regions colocalized with diI-LDL. The FITC-Tf in Fig. 3f, colocalized with the diI-LDL spots in Fig. 3e, are shown in Fig. 3g. The mean FITC-Tf power per region, or the sum of the FITC-Tf powers per field, normalized to the number of cells, was also measured. The number of diI-LDL spots and their mean power were determined as described previously (Dunn et al., 1989; Dunn and Maxfield, 1992).

^{125}I-transferrin experiments

^{125}I-Tf was prepared as described previously (Yamashiro et al., 1984). For the ^{125}I-Tf experiments, the labeling medium was 3 μg/ml ^{125}I-Tf in McCoy's 5A medium supplemented with 2 mg/ml ovalbumin, and experiments were done on monolayers of cells grown in six-well plates. To check for ^{125}I-Tf binding specificity, control experiments were done in the presence of 200 times excess of unlabeled Tf.

Tf exit from HEp2 cells was measured as described previously

(McGraw and Maxfield, 1990). In short, cells were incubated for ~1.5 hours at 37°C with 3 μg/ml ^{125}I-Tf in labeling medium. A pH 4.6 mild acid/neutral wash was then used to remove the cell surface transferrin, and the cells were chased for different lengths of time in chase medium. The chase medium was removed, the cells were solubilized in 0.1 M NaOH, and the radioactivity was counted in a gamma counter.

The steady-state ratio of Tf on the surface of HEp2 cells to Tf inside was determined, as previously described, from the surface and total cell-associated ^{125}I-Tf (McGraw and Maxfield, 1990). The surface Tf was obtained by incubating cells for 2 hours at 4°C with 3 μg/ml ^{125}I-Tf in medium 1. After extensive washing with cold medium 1, the cells were solubilized and counted. To determine the total amount of cell-associated Tf, cells were incubated at 37°C with 3 μg/ml ^{125}I-Tf in labeling medium for 2 hours, rinsed several times in chase medium, and then solubilized and counted.

RESULTS

Transferrin exit and internalization in HEp2 cells

We first quantified Tf internalization and exit in HEp2 cells. To measure Tf recycling rates directly, HEp2 cells were labeled to steady-state Tf receptor occupancy with ^{125}I-Tf, the Tf remaining on the surface was stripped with an acid rinse, and the cells were then chased for various times. As shown in Fig. 1 (filled circles) the decay in cell-associated ^{125}I-Tf over time was fit by a single exponential function, giving a rate constant for Tf efflux, k_e, of 0.105±0.005 min^{-1}, which corresponds to a half-time of about 6.6 minutes.

To determine whether our fluorescence imaging and image quantification techniques were consistent with our biochemical assays, we measured FITC-Tf exit from HEp2 cells. Cells were incubated for 1 hour with FITC-Tf, followed by an acid wash, and chased for various times. The total FITC-Tf power, normalized for the number of cells present, was determined for each field and the results from two experiments are plotted in Fig. 1 (open symbols). These experiments show that our image quantification techniques are reliably able to measure FITC-Tf trafficking.

The rate of Tf accumulation inside a cell, assuming first-order kinetics, is:

$$\frac{dT_C}{dt} = k_i T_P - k_e T_C, \quad (1)$$

where T_P is the Tf concentration on the plasma membrane, T_C is the Tf concentration inside the cell, k_i is the Tf internalization rate constant, and k_e is the rate of Tf exit from inside the cell. At steady-state, the labeled Tf concentration in cells does not change (i.e. $dT_C/dt=0$), so:

$$k_i = k_e \frac{T_C}{T_P}. \quad (2)$$

The steady-state value of T_P/T_C was measured to be 0.629±0.011 over 4 separate experiments. Thus, using equation (2) with a k_e of 0.105 min^{-1}, the Tf internalization rate constant would be 0.167±0.009 min^{-1}.

Transferrin uptake in HEp2 cells

We next identified the structures that Tf passes through in HEp2 cells, by incubating the cells for various times with saturating concentrations of FITC-Tf. The cells were also labeled with diI-LDL during the last 4 minutes of the FITC-Tf labeling. If the FITC-Tf labeling was less than 4 minutes, the diI-LDL was applied before the FITC-Tf. Comparison of the FITC-Tf labeling with the 4 minute diI-LDL-labeled endosomes indicated whether the FITC-Tf had sorted from diI-LDL towards its recycling route. Images from this experiment are shown in color in Fig. 2, and in black and white in Fig. 3.

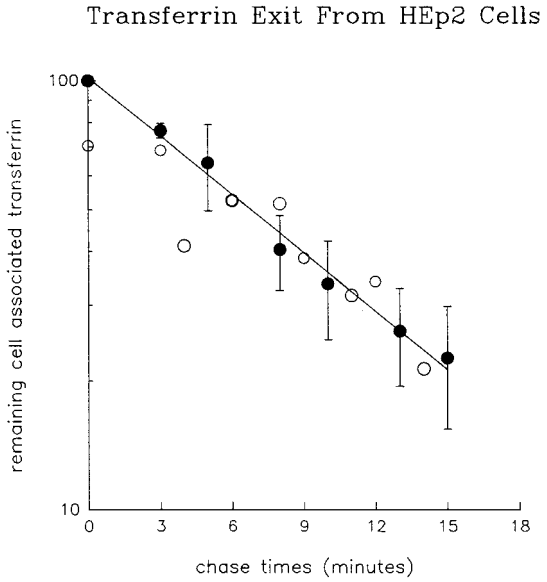

Fig. 1. Transferrin exit from HEp2 cells. HEp2 cells were labeled to steady-state with 3 μg/ml ^{125}I-Tf, acid washed to remove cell surface Tf, and then chased for various times. The cells were then solubilized, counted in a gamma counter, and the means from 8 separate experiments were plotted (●). The decrease in the amount of cell-associated ^{125}I-Tf over time was fit by a single exponential decay (continuous line), giving a ^{125}I-Tf exit rate of 0.105±0.005 min^{-1}. In separate experiments, HEp2 cells were labeled to steady state with 5 μg/ml FITC-Tf, acid washed to remove cell surface Tf, and then chased for various times. The images were used to quantify the FITC-Tf power per cell, and the means from 2 experiments (5 separate fields of cells per time point for each experiment) were plotted (○). The FITC-Tf decrease in cells showed similar kinetics to the ^{125}I-Tf decrease. Error bars are s.d.

Fig. 3b is a projection of a vertical stack of images showing HEp2 cells after a 1 minute incubation with FITC-Tf. A projection of the same field of cells showing 4 minute diI-LDL-labeled structures is in Fig. 3a. Most of the FITC-Tf was in punctate spots, which colocalized with the 4 minute diI-LDL-labeled endosomes, implying that they were in the same structure. This also means that these 4 minute diI-LDL endosomes were still fusion-accessible to endocytic vesicles and able to receive newly endocytosed FITC-Tf.

HEp2 cells incubated with FITC-Tf for 3 minutes are shown in Fig. 3d, and the same field of cells showing the location of 4 minute diI-LDL-labeled endosomes is shown in Fig. 3c. The color version of this image showing both probes simultaneously is Fig. 2a, where most of the diI-LDL spots (red) contain FITC-Tf (green) giving these colocalized spots an orange-yellow appearance (see arrows in Figs 2a,b and 3c,d). By 3 minutes, some of the spots containing both diI-LDL and FITC-Tf also showed FITC-Tf extensions (in green) beyond the region solely labeled by diI-LDL. To see the extensions from diI-LDL spots more clearly, the lower left region of Fig. 2a is

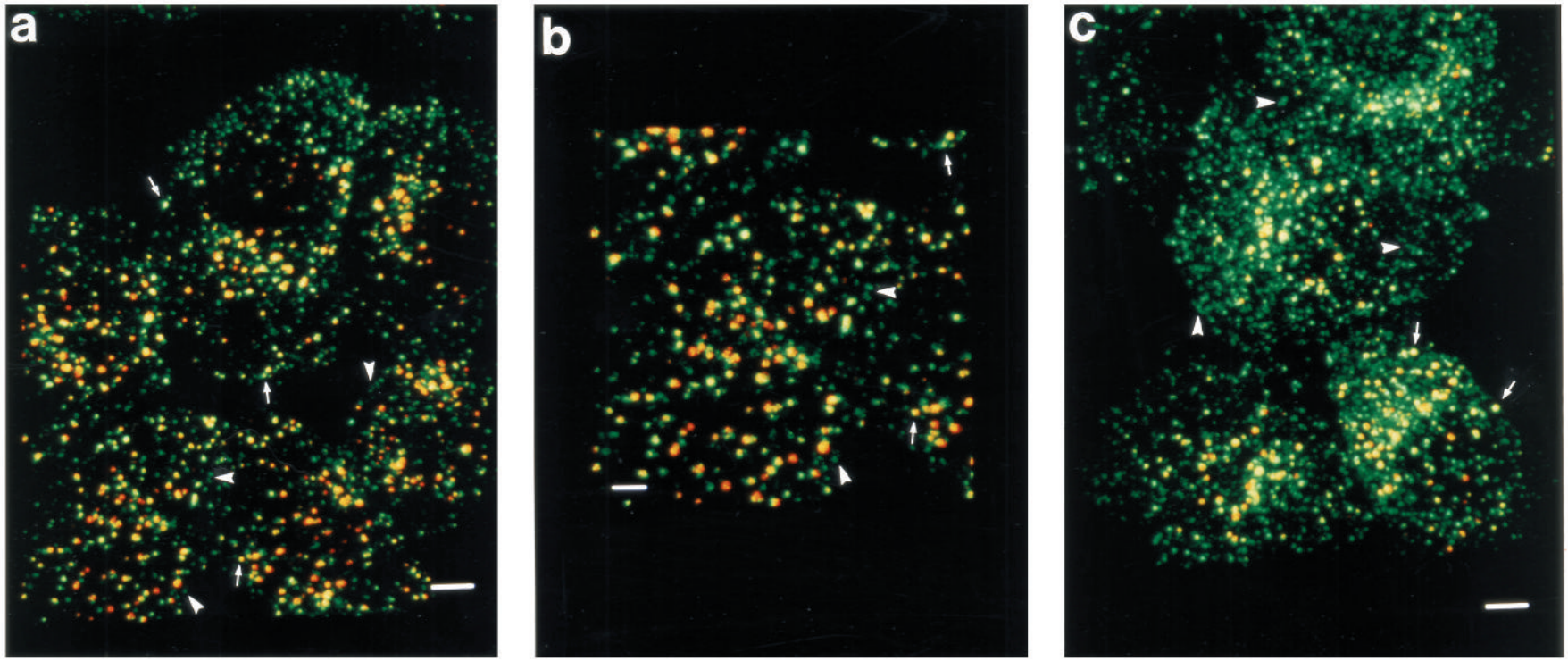

Fig. 2. FITC-Tf accumulation in HEp2 cells. HEp2 cells were incubated with 5 μg/ml FITC-Tf (green) for 3 minutes (a and b), or 8 minutes (c), fixed, and observed by confocal fluorescence microscopy. For the 4 minutes prior to fixation, cells were also incubated with 20 μg/ml diI-LDL (red) to label endosomes. Each image is a projection of a vertical stack of images of the whole cell. After 3 minutes (a and b), most of the FITC-Tf was coincident with diI-LDL spots as shown by yellow-orange areas where they overlap (arrows). There are also some dimmer FITC-Tf-labeled structures that did not contain diI-LDL (arrowheads). The lower left part of a is shown enlarged in b, and some of the double-labeled organelles appear to have extensions that contain only FITC-Tf. After 8 minutes (c) the FITC-Tf labeled either punctate structures containing diI-LDL (arrows), or structures lacking diI-LDL (arrowheads). Bars: 5 μm, a and c; 2.5 μm, b.

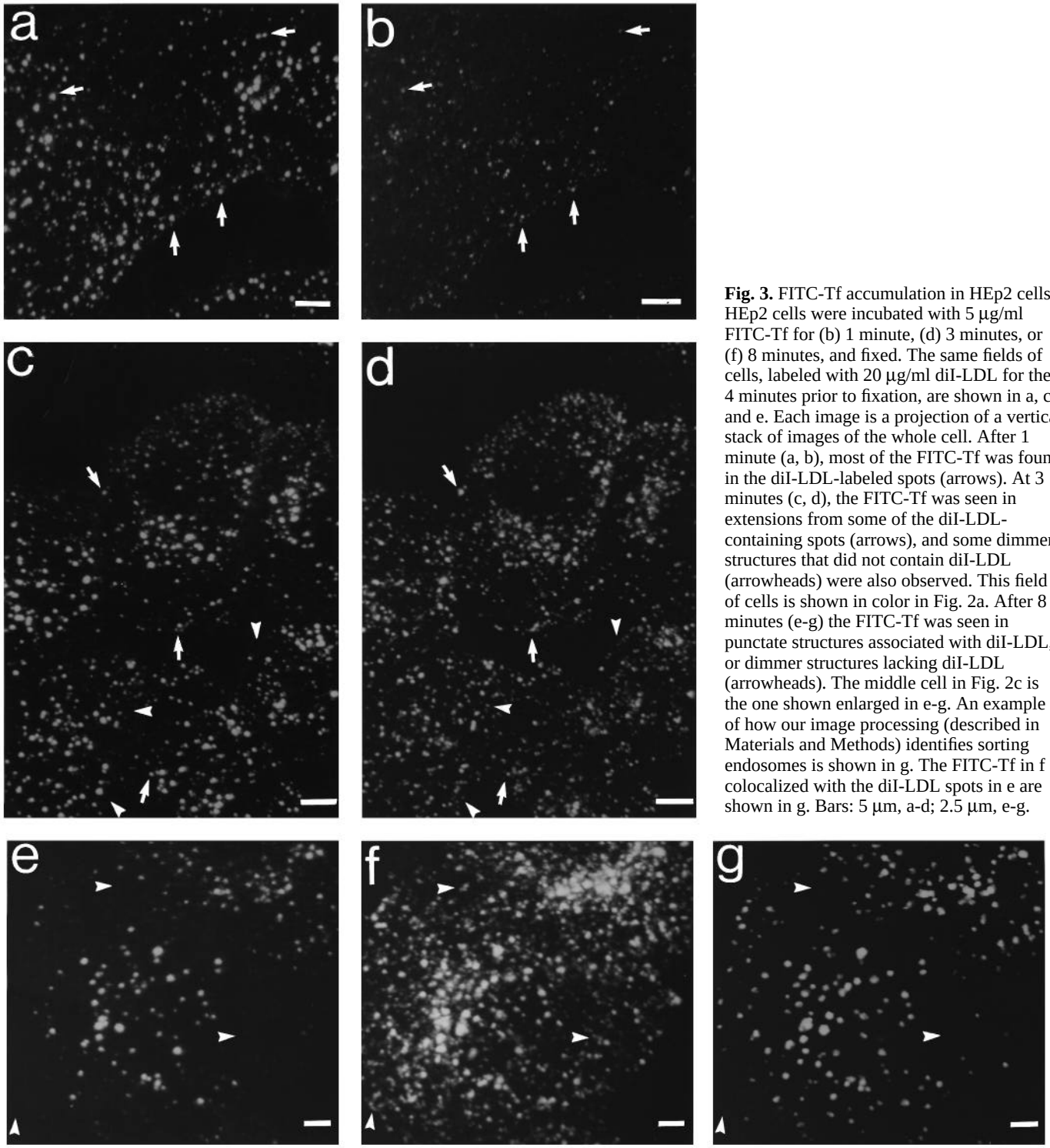

Fig. 3. FITC-Tf accumulation in HEp2 cells. HEp2 cells were incubated with 5 μg/ml FITC-Tf for (b) 1 minute, (d) 3 minutes, or (f) 8 minutes, and fixed. The same fields of cells, labeled with 20 μg/ml diI-LDL for the 4 minutes prior to fixation, are shown in a, c and e. Each image is a projection of a vertical stack of images of the whole cell. After 1 minute (a, b), most of the FITC-Tf was found in the diI-LDL-labeled spots (arrows). At 3 minutes (c, d), the FITC-Tf was seen in extensions from some of the diI-LDL-containing spots (arrows), and some dimmer structures that did not contain diI-LDL (arrowheads) were also observed. This field of cells is shown in color in Fig. 2a. After 8 minutes (e-g) the FITC-Tf was seen in punctate structures associated with diI-LDL, or dimmer structures lacking diI-LDL (arrowheads). The middle cell in Fig. 2c is the one shown enlarged in e-g. An example of how our image processing (described in Materials and Methods) identifies sorting endosomes is shown in g. The FITC-Tf in f colocalized with the diI-LDL spots in e are shown in g. Bars: 5 μm, a-d; 2.5 μm, e-g.

zoomed and shown in Fig. 2b. In some instances FITC-Tf appeared in dimmer structures that did not have any connections to the diI-LDL labeled spots, as seen by the arrowheads marking the presence of FITC-Tf in Figs 2a,b and 3d, and the absence of diI-LDL at the same locations in Fig. 3c.

At 8 minutes (Fig. 2c), FITC-Tf was still in structures that had some overlap with diI-LDL (arrows), but it was also found in dimmer, extensive areas that did not colocalize with diI-LDL (arrowheads). The FITC-Tf in diI-LDL-containing spots had extensions that often appeared as tubules extending from them. The dimmer FITC-Tf structures (arrowheads) were often seen to be clearly separated from the bright FITC-Tf-labeled tubules contiguous with the diI-LDL spots. Some, but not all of these dimmer FITC-Tf structures seemed to be made up of tubular structures. Occasionally the dim structures touched the FITC-Tf tubules contiguous with diI-LDL-containing regions,

but it was not clear if they were truly connected, or if their separation was smaller then the light microscope's resolution.

To illustrate further the two types of FITC-Tf-labeled structures (attached to diI-LDL spots, or separate), the middle cell in Fig. 2c is shown enlarged with the diI-LDL distribution in Fig. 3e and the FITC-Tf labeling in Fig. 3f. In several regions of this cell there were no diI-LDL-labeled spots nearby (within ~2-5 μm), so the separation of the dim FITC-Tf structures from diI-LDL-containing spots is more clearly seen. These dim FITC-Tf structures are marked by arrowheads in Fig. 3f, and the same locations in Fig. 3e are marked to show the absence of diI-LDL. Occasionally, bright FITC-Tf-containing structures are seen without any diI-LDL fluorescence; this can be either due to the diI-LDL present not being bright enough for detection, or because the FITC-Tf-containing structure lacks diI-LDL but is brightly labeled with FITC-Tf in this instance.

Based on these observations, the Tf-containing endosomes in HEp2 cells can be subdivided as in CHO cells (Dunn et al., 1989; Dunn and Maxfield, 1992; Mayor et al., 1993). Sorting endosomes contain newly endocytosed LDL and Tf, and can be identified as the structures in Figs 2 and 3 labeled with both diI-LDL and FITC-Tf. The FITC-Tf also labeled the tubular extensions of the sorting endosome. The FITC-Tf then exited the sorting endosomes and entered the dimmer recycling compartment, which appeared as a separate compartment from the diI-LDL-containing sorting endosomes in Figs 2 and 3.

FITC-Tf and diI-LDL accumulation kinetics

To determine the kinetics of Tf entry into sorting endosomes and the whole cell we quantified their FITC-Tf fluorescence from images similar to those shown in Fig. 3. The FITC-Tf accumulation in cells at various times was determined by measuring the total FITC-Tf power in each projection image and then normalizing for the number of cells present. The results from three experiments were normalized to the 3 minute value (which was a common time point for the data sets), averaged, and plotted in Fig. 4a.

The total cell-associated Tf, T_T, is the sum of the plasma membrane Tf and the Tf inside the cell. In the case of continuous saturable Tf labeling, the Tf concentration on the plasma membrane, T_P, is a constant, and the rate of Tf accumulation inside a cell is given by equation (1). Solving equation (1) gives the Tf concentration in a cell during continuous saturable ligand binding (T_P constant) as:

$$T_C(t) = T_P \frac{k_i}{k_e}[1 - e^{-k_e t}]. \quad (3)$$

The total FITC-Tf in a cell versus time, shown in Fig. 4a, was fit by:

$$T_T(t) = A[1 - e^{-k_e t}] + B, \quad (4)$$

where the three parameters fit were the asymptotic value A, the detected Tf amount on the plasma membrane B, and k_e. The best fit gave a value for k_e of 0.13±0.05 min^{-1}, corresponding to a half-time for Tf to exit the cell of 5.3 minutes. The Tf exit rates determined here were faster than those obtained from directly measuring Tf exit in cells labeled to steady state ($t_{\frac{1}{2}}$ ~6.6 minutes; Fig. 1), but the difference was not statistically significant.

Tf in a vectorial pathway goes from the plasma membrane to sorting endosomes to recycling compartments and then back to the plasma membrane (see schematic diagram in Fig. 8), and the rate of Tf accumulation in sorting endosomes in such a scheme is:

$$\frac{dT_S}{dt} = k_i T_P - k_S T_S, \quad (5)$$

where T_S is the Tf concentration in sorting endosomes, and k_s is the sorting rate constant. This was solved, for the case of saturable continuous Tf labeling, where T_P is a constant. Thus, the Tf in sorting endosomes from a vectorial trafficking pathway is:

$$T_S(t) = C[1 - e^{-k_S t}]. \quad (6)$$

We quantified FITC-Tf accumulation in sorting endosomes. Sorting endosomes were defined as structures where FITC-Tf and diI-LDL were colocalized. As seen in Figs 2 and 3, FITC-Tf in sorting endosomes was not only in the punctate spots labeled by diI-LDL but also in their tubular extensions. However, there was no unambiguous way to identify the tubular extensions that were connected to diI-LDL spots. Thus we only measured the FITC-Tf power contained within areas colocalized with the diI-LDL spots. Fig. 3e-g demonstrates what our image processing routines select as the colocalized diI-LDL- and FITC-Tf-containing regions. The FITC-Tf regions of Fig. 3f colocalized with the diI-LDL spots of Fig. 3e are shown in Fig. 3g.

The mean FITC-Tf value over all the diI-LDL spots was determined and fitted with the expression for T_S, where the two quantities fit were the sorting rate constant, k_S and the asymptotic value C. The mean FITC-Tf power in diI-LDL spots was then normalized by the value of the asymptote. This was done so that results from the two experiments could be averaged. The FITC-Tf powers in sorting endosomes after various incubation times are plotted in Fig. 4b along with the optimal fit of the data using equation (6). The k_S for FITC-Tf colocalized with diI-LDL spots was 0.26±0.13 min^{-1}, corresponding to a half-time of exit from sorting endosomes of 2.7 minutes.

We next examined diI-LDL accumulation in endosomes by incubating HEp2 cells for different lengths of time with diI-LDL. The mean diI-LDL power per spot increased up to 12 minutes, after which it leveled off (Fig. 4c). The line connecting the points in Fig. 4c is a spline fit through the data.

The relative increase in the amount of diI-LDL in spots was much larger than that of FITC-Tf, suggesting that FITC-Tf is removed from sorting endosomes while diI-LDL continues to accumulate. The half-time for Tf to leave sorting endosomes was 2-3 minutes, but the half-time for it to leave the cell was 5-8 minutes (Table 1). This implies that after leaving sorting endosomes, Tf must accumulate in a separate compartment, the recycling compartment, before exiting the cell.

Sorting of FITC-Tf from diI-LDL in sorting endosomes

To directly study Tf sorting from LDL in sorting endosomes, HEp2 cells were labeled with a 2 minute pulse of FITC-Tf and diI-LDL. The surface Tf was removed by acid stripping, followed by chases of various times. A projection of a vertical stack of HEp2 cells labeled in this manner for 2 minutes with FITC-Tf and diI-LDL, acid washed for 2 minutes and then chased for 1 minute is shown in Fig. 5a and b. The diI-LDL-

labeled spots contained FITC-Tf (i.e. they were sorting endosomes), and there was also some FITC-Tf in dim structures not associated with diI-LDL (i.e. recycling compartments). Another field of cells labeled in the same way, but now chased for 3 minutes, is shown in Fig. 5c and d. The amount of FITC-Tf in diI-LDL endosomes had decreased (see arrows), and regions not associated with diI-LDL clearly showed FITC-Tf staining (see arrowheads). The FITC-Tf in diI-LDL endosomes in Fig. 5d is ~55% of the FITC-Tf in diI-LDL endosomes in Fig. 5b. The total FITC-Tf in the cells in Fig. 5d is ~80% of the total FITC-Tf in the cells in Fig. 5b, and this total cellular FITC-Tf decrease is consistent with the previously measured exit rate, k_e.

The FITC-Tf in each diI-LDL spot was quantified by image processing, and the mean FITC-Tf power per diI-LDL spot, for all the diI-LDL spots, was plotted versus chase times (following the 2 minute acid wash) in Fig. 6. The mean FITC-Tf power in diI-LDL spots had a single exponential decrease over chase times, implying that Tf sorted from LDL with first-order kinetics. The sorting rate constant, k_S, was obtained from a single exponential fit of the plot and is 0.28±0.04 min^{-1}, giving a 2.5 minute half-time for FITC-Tf sorting from diI-LDL. This sorting rate constant was in the same range as that obtained from the Tf accumulation data. Similar sorting half-times were seen in two other experiments of this kind (~1.8 and 2.3 minutes). Taken together with the analyses of accumulation kinetics, these sorting data indicate that Tf exits sorting endosomes with a $t_{\frac{1}{2}}$ of ~2.5 minutes (Table 2).

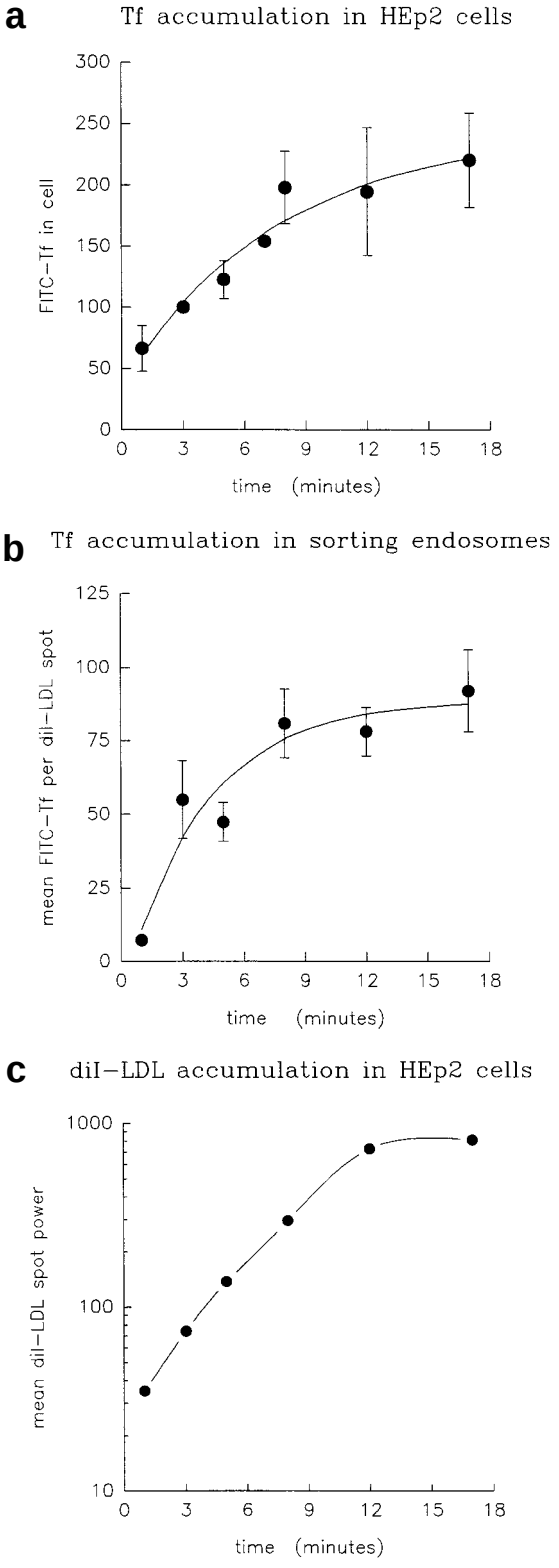

Sorting endosomes mature into late endosomes

It has been shown that delivery of ligands from sorting endosomes to late endosomes in CHO cells occurs by the mat-

Table 1. Summary of measured transferrin and LDL trafficking rate constants

Trafficking step	Parameter	Rate constant ±s.e. (min^{-1})	Half-time (min)
^{125}I-Tf exit from inside the cell measured directly (Fig. 1)	k_e	0.105±0.005	6.6
FITC-Tf exit from inside the cell measured directly (Fig. 1)	k_e	0.09±0.01	7.7
FITC-Tf exit from inside the cell measured from accumulation kinetics (Fig. 4a)	k_e	0.13±0.05	5.3
FITC-Tf exit from diI-LDL spots measured directly (Fig. 6)	k_S	0.28±0.04	2.5
FITC-Tf exit from diI-LDL spots measured from accumulation kinetics (Fig. 4b)	k_S	0.26±0.13	2.7
Sorting endosome maturation (Fig. 7a)	k_m	0.04±0.01	17
Transferrin internalization (using k_e=0.105 min^{-1})	k_i	0.167±0.009	4.2

Fig. 4. Quantification of FITC-Tf and diI-LDL accumulation in HEp2 cells. (a) The FITC-Tf power per HEp2 cell versus time was measured from images collected in experiments similar to those depicted in Figs 2 and 3. The mean from 3 experiments (5 separate fields of cells per time point for each experiment) was fit with the expression for total cell-associated Tf (eqn 4), and gave a Tf exit rate, k_e, of 0.13±0.05 min^{-1}. (b) The FITC-Tf power in 4 minute diI-LDL-labeled spots was measured in images from five separate fields of cells recorded at each time point for 2 experiments similar to Fig. 2. The data were fit by equation (6), which describes Tf accumulation in sorting endosomes with 1st-order kinetics, and gave a rate constant, k_S, for FITC-Tf to leave diI-LDL spots, of 0.26±0.13 min^{-1}. (c) HEp2 cells were incubated with 20 μg/ml diI-LDL for different times, and the mean diI-LDL power per spot (from 5 separate fields of cells per time point) was measured as described in the text. Error bars in a are the s.d. between experiments, and in b are the s.d. from all 10 fields of the 2 experiments.

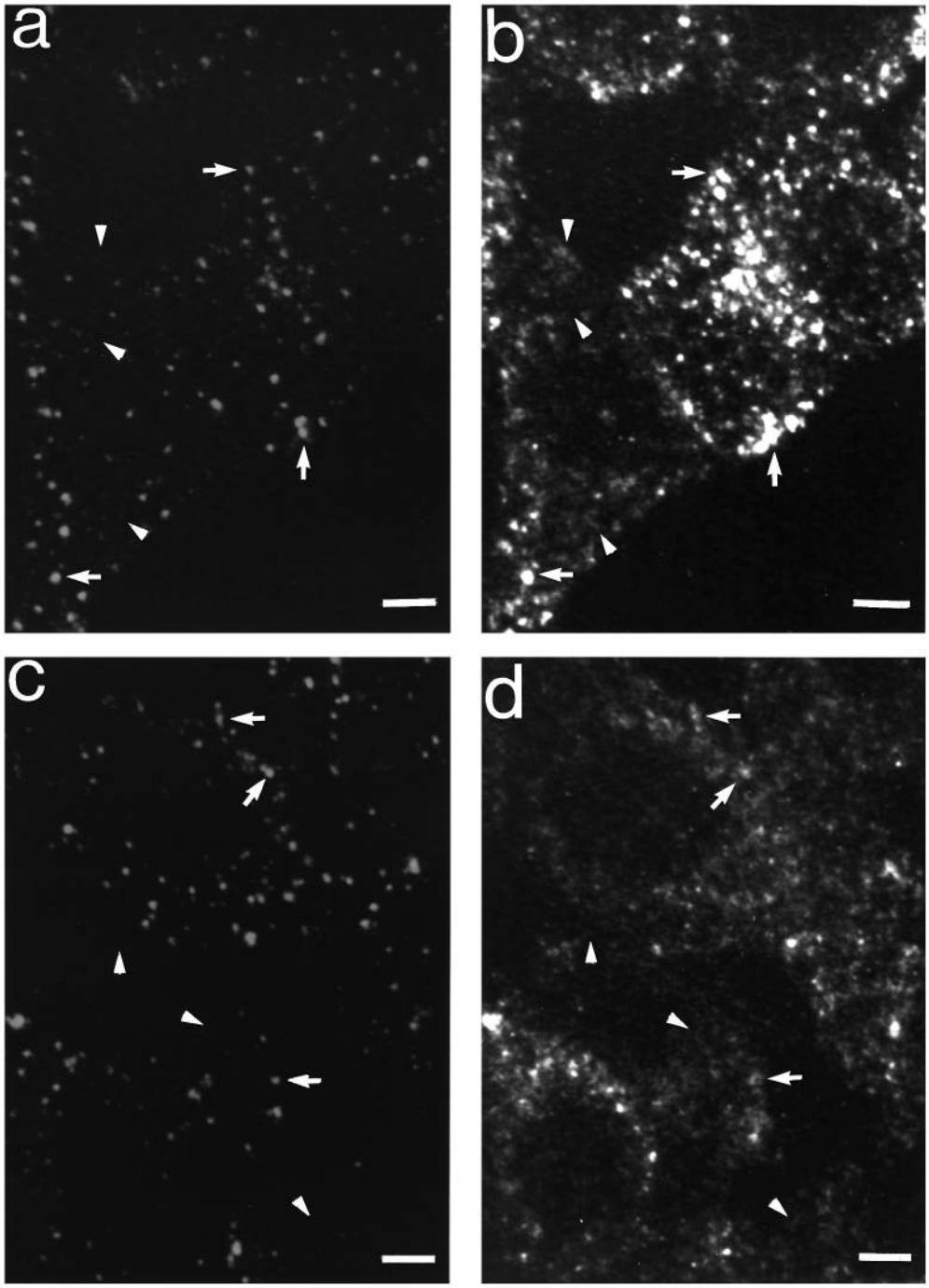

Fig. 5. Sorting of FITC-Tf from diI-LDL. HEp2 cells were pulsed for 2 minutes with 20 μg/ml diI-LDL and FITC-Tf. The cell surface Tf was removed by a 2 minute acid wash, and then chased for 1 minute (a and b) or 3 minutes (c and d). DiI-LDL labeling is shown in a and c, and FITC-Tf labeling is shown in b and d. Each image is a projection of a vertical stack of images of the whole cell. After 1 minute chase (a, b) most of the diI-LDL spots still contained FITC-Tf (arrows), although some FITC-Tf staining was seen in dim filamentous areas not associated with the diI-LDL spots (arrowheads in a and b). After a 3 minute chase (c, d) less FITC-Tf was in diI-LDL dots (arrows), and the dim structures not associated with diI-LDL are more clearly seen (arrowheads). Bar, 5 μm.

uration of sorting endosomes (Dunn et al., 1989; Salzman and Maxfield, 1989; Dunn and Maxfield, 1992). To demonstrate this, cells were pulsed with diO-LDL (which fluoresces green), and after variable chases given a brief pulse of diI-LDL (which fluoresces red) to label sorting endosomes. If sorting endosomes convert to late endosomes by a maturation process, the diO-LDL content in diI-LDL-labeled sorting endosomes would remain constant over chase times. By contrast, if molecules sorted to late endosomes from a stable early endosomal compartment, the diO-LDL content per sorting endosome would decrease due to removal by shuttle vesicles. Additionally, in a maturation process the fraction of endosomes labeled with diO-LDL that are accessible by diI-LDL would decrease over time, consistent with the diO-LDL-labeled endosomes losing their ability to receive newly endocytosed diI-LDL and maturing into late endosomes.

We carried out pulse-chase-pulse experiments on HEp2 cells to see if endocytic ligand delivery to late endosomes also occured by sorting endosome maturation in these cells. HEp2 cells were incubated with a 3 minute pulse of diO-LDL followed by variable chases and then a 2 minute pulse of diI-LDL, an additional 2 minute chase and fixation. Cells were imaged by confocal microscopy, and projections of the confocal slices were made. The ligand content per sorting

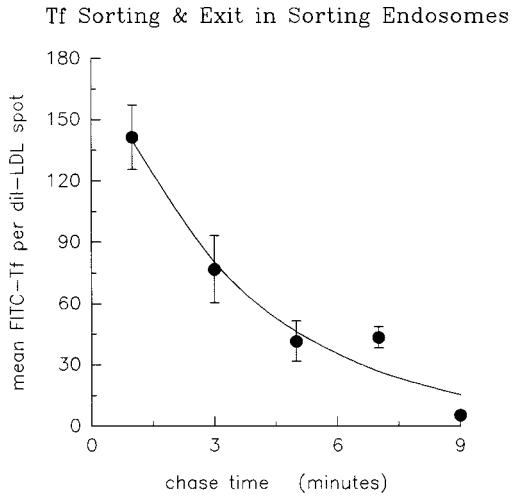

Fig. 6. Sorting kinetics of FITC-Tf from diI-LDL. The images from the experiments described in Fig. 5 were quantified for the mean amount of FITC-Tf in diI-LDL spots (from 5 separate fields of cells recorded at each time point). The FITC-Tf decrease in diI-LDL spots was well fit with a single exponential decay giving a rate constant of 0.28±0.04 min^{-1}. Error bars are s.d.

Table 2. Trafficking half-times for HEp2 and TRVb-1 (CHO) cells

Trafficking step	Symbol used	Half-time in HEp2 cells (min)	Half-time in TRVb-1 (CHO) cells (min)
Transferrin/LDL sorting	k_S	~2.5	2[a]
Transferrin exit from cells	k_e	~7	9[b]-12[c]
Transferrin internalization	k_i	~4	6[c]
Sorting endosome maturation	k_m	~17	6[d]-8[e]

[a]Dunn et al. (1989); Mayor et al. (1993).
[b]Mayor et al. (1993); Presley et al. (1993).
[c]McGraw and Maxfield (1990).
[d]Dunn and Maxfield (1992).
[e]Salzman and Maxfield (1988); Salzman and Maxfield (1989).

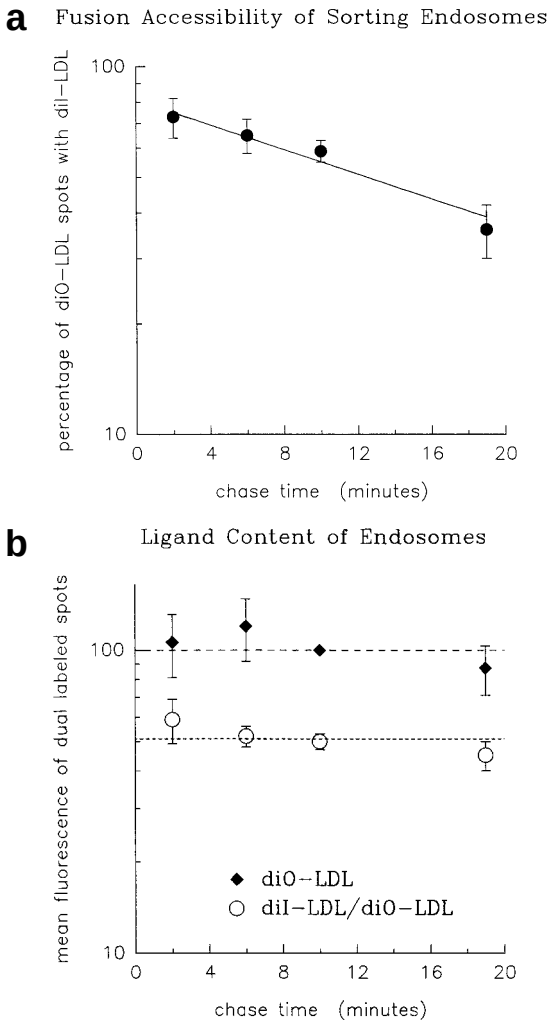

Fig. 7. Sorting endosome maturation. HEp2 cells were pulsed for 2 minutes with 20 μg/ml diO-LDL, followed by variable chases and then a 2 minute pulse of 2 μg/ml diI-LDL. The fusion accessibility of sorting endosomes is demonstrated in a, which shows the percentage of diO-LDL-labeled spots that were also labeled by diI-LDL, as a function of the chase time. This decreased over time, and when fit with an exponential, gave a decay rate of 0.04±0.01 min^{-1}. The amount diO-LDL in dual-labeled spots was relatively constant over time, as shown in b. The ratio of diI-LDL to diO-LDL was also constant over time, implying that maturation was a sudden rather than a gradual event. The data were means from 3 experiments, each with 5 separate fields of cells per time point. Error bars are s.d.

endosome and the fraction of endosomes labeled with diO-LDL and still accessible to diI-LDL were assessed, as done previously (Dunn and Maxfield, 1992).

Fig. 7a shows the percentage of diO-LDL-labeled endosomes that were labeled with diI-LDL. This decreased over time, and when fit to a single exponential function, gave a rate constant of 0.04±0.01 min^{-1} ($t_{\frac{1}{2}}$ ~17 minutes). The mean amount of diO-LDL per dual-labeled sorting endosome was constant over chase times, as shown in Fig. 7b. These results indicate that sorting endosomes in HEp2 cells lost the ability to receive newly endocytosed material, and matured into late endosomes with a ~17 minute half-time. This behavior is similar to that of CHO cells (6-8 minute maturation half-time; Dunn and Maxfield, 1992).

Stoorvogel et al. (1991) have suggested that maturation is a gradual event. If sorting endosomes lost their ability to receive newly endocytosed LDL gradually, then the mean diI-LDL (second probe) per diO-LDL-containing endosome would be expected to decrease over time. However, Fig. 7b also shows that the ratio of diI-LDL to diO-LDL over chase times was fairly constant, implying a rapid loss in the ability of the diO-LDL-labeled sorting endosomes to accept newly endocytosed diI-LDL in HEp2 cells. Similar results were obtained by Dunn and Maxfield (1992) with CHO cells. These interpretations of our results are based on the assumption that, since the diI-LDL and diO-LDL pulse times (2 and 3 minutes) are short compared to the half-time for maturation (17 minutes), few sorting endosomes would mature during either of the pulse times. Thus the constant ratio of diI-LDL to diO-LDL over chase times in Fig. 7b is due to a relatively rapid maturation step where a constant amount of diI-LDL and diO-LDL was delivered to the endosomes during each of the two pulses.

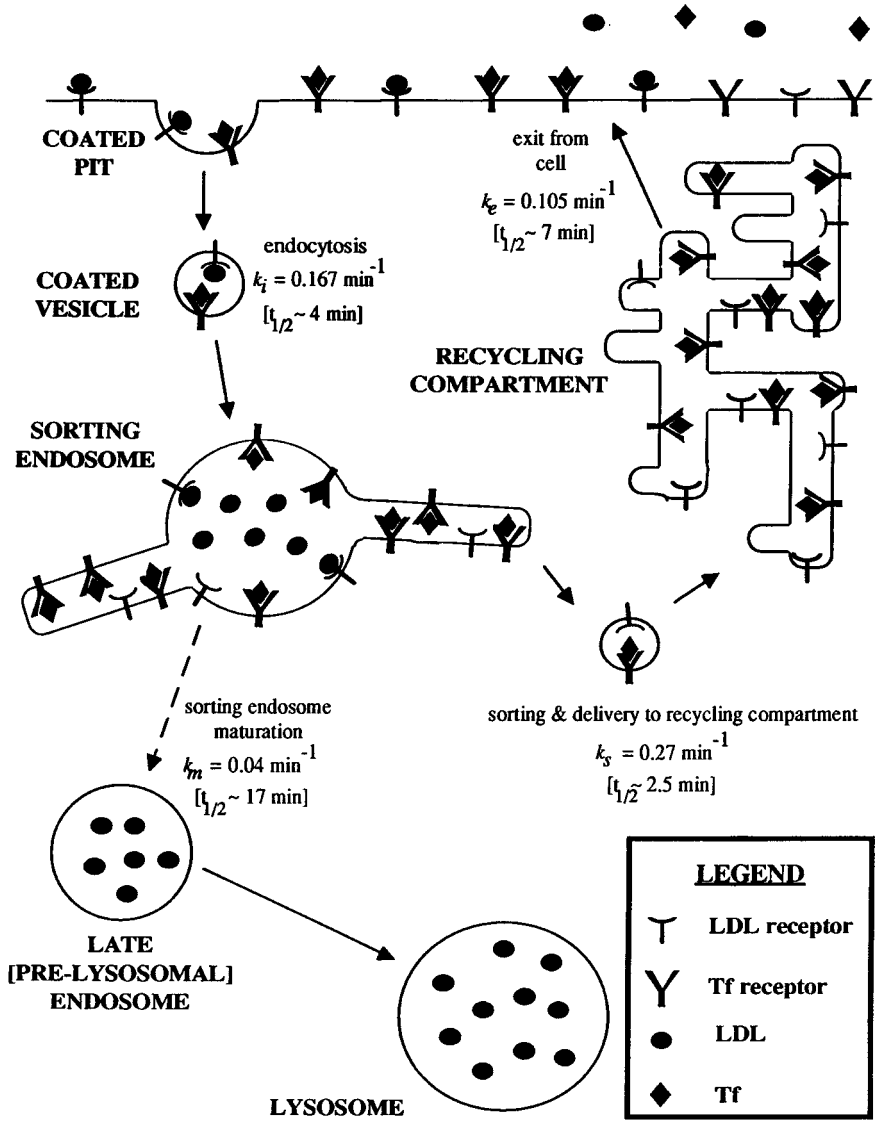

Fig. 8. Schematic diagram of Tf and LDL trafficking in HEp2 cells. Tf and LDL are internalized by their respective receptors in coated pits. They are delivered to sorting endosomes via coated vesicles where the LDL comes off its receptor and accumulates in the bulk volume. Tf, still bound to its receptor, and the LDL receptor, are distributed along the membrane area of the sorting endosome, and its tubular extensions. Tf and LDL sort with a half-time of ~2.5 minutes. Tf and the LDL receptor are then delivered to the recycling compartment, and exit the cell with a ~7 minute half-time. The sorting endosomes, containing the accumulated LDL, lose their ability to receive newly endocytosed material and mature into late endosomes with a ~17 minute half-time.

DISCUSSION

Our observations and measurements of Tf and LDL trafficking in HEp2 cells have demonstrated that the Tf-containing endosomes in these cells are composed of two separate compartments: the sorting endosome and the recycling compartment. We have presented both morphological and kinetic evidence supporting this conclusion. Endocytosed Tf and LDL were initially internalized into the same punctate tubulo-vesicular compartments (sorting endosomes). Tf then exits the LDL-containing sorting endosomes and starts appearing in a separate compartment, the recycling compartment. The rates for Tf and LDL sorting and trafficking, measured by various methods, are shown in Table 1. Table 2 summarizes the rounded $t_{\frac{1}{2}}$ values obtained from the weighted means for the various values of k_e and k_S. Tf sorted from LDL with first-order kinetics gave a $t_{\frac{1}{2}}$ of ~2.5 minutes. However, Tf cycled through the cell with a half-time of ~7 minutes. The difference in the two half-times implies that Tf is delivered to a separate compartment (recycling compartment) after leaving the LDL-labeled sorting endosome, but before exiting the cell. Sorting endosomes eventually stop receiving newly endocytosed LDL, and rapidly mature into late endosomes. The time for half of the sorting endosomes to mature was found to be ~17 minutes. Fig. 8 shows a schematic diagram summarizing these results.

Transferrin trafficking in HEp2 cells follows the same general scheme as in CHO cells. Table 2 compares the rate constants for HEp2 cells and TRVB-1 cells, a CHO cell line expressing the human Tf receptor (McGraw et al., 1987; McGraw and Maxfield, 1990). As discussed in the Introduction, a wealth of evidence has shown that the compartments that Tf traffics through in CHO cells consist of separate, distinct sorting endosomes and recycling compartments (Yamashiro et al., 1984; Dunn et al., 1989; Mayor et al., 1993; McGraw et al., 1993; Presley et al., 1993). These compartments are morphologically different; the sorting endosomes are tubulo-vesicular structures, but the recycling compartment is a condensed tubular organelle in the peri-centriolar region of the cell. In HEp2 cells, Tf and LDL initially enter tubulo-vesicular structures that function as sorting endosomes, since Tf is rapidly removed whereas LDL is retained. After leaving the sorting endosomes, Tf enters a recycling compartment that

appears as dimly fluorescent organelles throughout the cell. Some, but not all of these appear to be tubular. Ligand delivery to late endosomes occurs by sorting endosome maturation (Dunn et al., 1989; Dunn and Maxfield, 1992).

It is our interpretation that the recycling compartment corresponds to at least some of the tubular endosomes seen by Hopkins et al. (1990) and by Tooze and Hollinshead (1991). After an extended labeling period, Hopkins et al. (1990) found extensive Tf-labeled tubular endosomes in HEp2 cells that were seen throughout the cell but did not form a continuous organelle. Tooze and Hollinshead (1991), using horseradish peroxidase (HRP) as a fluid-phase marker, also found tubular endosomes in HEp2 cells when thick sections were viewed by electron microscopy. They found that in HEp2 cells tubular endosomes received HRP within 5 minutes, but at least 30 minutes were needed to label the entire tubular endosomal system. They also saw tubular endosomes that were not in the vicinity of cisternal-vesicular early endosomes, which would be consistent with our interpretation that the recycling compartment is distinct from the sorting endosomes. The kinetics, temperature sensitivity and microtubule insensitivity of HRP entering and leaving tubular endosomes identified them as early endocytic elements, and not late endosomes.

Hopkins and his colleagues (Futter and Hopkins, 1989; Hopkins et al., 1990) also reported that Tf and EGF trafficked together for long periods of time in HEp2 cells, and both appeared in multi-vesicular bodies (MVB), although Tf was on the perimeter membrane of MVB while EGF receptors increasingly appeared in the inner vesicles of MVB. Although EGF is a lysosomally directed ligand, they found that after a 10 minute pulse and a 30 minute chase, 40% of the EGF was in the same compartment as Tf, whereas our lysosomally directed probe, LDL, would clearly have been in different compartments by this time. Thus, it is not clear that EGF follows the same endocytic route in HEp2 cells as other lysosomally destined molecules such as LDL.

van Deurs et al. (1993) observed endosomes in HEp2 cells, using fluorescent Tf and video microscopy as well as HRP and cationized gold in electron microscopy. They observed vesicular endosomes with short tubular projections, and they found that these vesicular endosomes matured into late endosomes in agreement with our pulse-chase experiments with LDL. van Deurs et al. (1993) observed that the older endosomes had more inner vesicles. With continuous HRP incubation, the number of labeled MVB increased, whereas with a 5 minute HRP pulse followed by either 10 or 25 minute chases, the number of labeled MVB remained constant. van Deurs et al. (1993) did not find extensive tubular endosomes. The reasons for this are not clear.

Using confocal fluorescence microscopy and digital image analysis, we have morphologically and kinetically shown that internalized Tf first appears in HEp2 cells in sorting endosomes. It then sorts from lysosomally directed LDL and appears in a post-sorting recycling compartment before leaving the cell. The LDL remains behind in sorting endosomes, which mature into late endosomes. This is the same scheme as has been shown for CHO cells. We believe that this is a general scheme for the trafficking of recycling molecules in cells, and this pathway involves short-lived sorting endosomes containing both recycling and lysosomally directed molecules, and a chronologically later, post-sorting recycling compartment that is a relatively permanent (or long-lived) organelle.

Additional pathways may exist in the cell in which smaller amounts of Tf receptors can participate. Some Tf can appear in the TGN; asialotransferrin receptor has been shown to be resialated in the TGN, although with very slow kinetics (Snider and Rogers, 1985; Stoorvogel et al., 1988). We also have recent evidence showing that a substantial amount of Tf participates in a retrograde non-vectorial pathway where it returns to sorting endosomes from recycling compartments, as shown in a separate paper (Ghosh and Maxfield, unpublished data). This retrograde Tf trafficking does not affect the values of the various rate constants for vectorial Tf trafficking that we have measured here (k_S and k_e) as these were determined from pulse-chase experiments that measured the dominant forward vectorial trafficking rate, and the retrograde trafficking effects would be detected only after long time incubations.

We thank Michael Hillmeyer for sustained help in computer-related matters, and Jeffrey Myers for making and providing the fluorescent LDLs. We also thank Kenneth Dunn, Satyajit Mayor, Timothy McGraw and John Presley for critically reading the manuscript. This work was supported by a fellowship from the New York Affiliate of the American Heart Association to R. N. Ghosh, and a National Insitutes of Health grant DK27083 to F. R. Maxfield.

REFERENCES

Brown, M. S. and Goldstein, J. L. (1986). A receptor-mediated pathway for cholesterol homeostasis. *Science* **232**, 34-47.

Cain, C. C., Sipe, D. M. and Murphy, R. F. (1989). Regulation of endocytic pH by the Na^+,K^+-ATPase in living cells. *Proc. Nat. Acad. Sci. USA* **86**, 544-548.

Dunn, K. W., McGraw, T. E. and Maxfield, F. R. (1989). Iterative fractionation of recycling receptors from lysosomally destined ligands in an early sorting endosome. *J. Cell Biol.* **109**, 3303-3314.

Dunn, K. W. and Maxfield, F. R. (1992). Delivery of ligands from sorting endosomes to late endosomes occurs by maturation of sorting endosomes. *J. Cell Biol.* **117**, 301-310.

Futter, C. E. and Hopkins, C. R. (1989). Subfractionation of the endocytic pathway: isolation of compartments involved in the processing of internalised epidermal growth factor-receptor complexes. *J. Cell Sci.* **94**, 685-694.

Ghosh, R. N. and Maxfield, F. R. (1994). Evidence for non-vectorial, retrograde transferrin trafficking in the early endosomes of Hep2 cells.

Goldstein, J. L., Basu, S. K. and Brown, M. S. (1983). Receptor-mediated endocytosis of low-density lipoprotein in cultured cells. *Meth. Enzymol.* **98**, 241-260.

Goldstein, J. L., Brown, M. S., Anderson, R. G. W., Russell, D. W. and Schneider, W. J. (1985). Receptor mediated endocytosis: concepts emerging from the LDL receptor system. *Annu. Rev. Cell Biol.* **1**, 1-39.

Harford, J. B., Casey, J. L., Koeller, D. M. and Klausner, R. D. (1991). Structure, function and regulation of the transferrin receptor: insights from molecular biology. In *Intracellular Trafficking of Proteins* (ed. C. J. Steer and J. A. Hanover), pp. 302-334. Cambridge University Press, Cambridge.

Hopkins, C. R., Gibson, A., Shipman, M. and Miller, K. (1990). Movement of internalized ligand-receptor complexes along a continuous endosomal reticulum. *Nature* **346**, 335-339.

Mattia, E., Rao, K., Shapiro, D. S., Sussman, H. H. and Klausner, R. D. (1984). Biosynthetic regulation of the human transferrin receptor by desferrioxamine in K562 cells. *J. Biol. Chem.* **259**, 2689-2692.

Maxfield, F. R. and Yamashiro, D. J. (1991). Acidification of organelles and the intracellular sorting of proteins during endocytosis. In *Intracellular Trafficking of Proteins* (ed. C. J. Steer and J. A. Hanover), pp. 157-182. Cambridge University Press, Cambridge.

Mayor, S., Presley, J. F. and Maxfield, F. R. (1993). Sorting of membrane components from endosomes and subsequent recycling to the cell surface occurs by a bulk flow process. *J. Cell Biol.* **121**, 1257-1269.

Mellman, I., Fuchs, R. and Helenius, A. (1986). Acidification of the endocytic and exocytic pathways. *Annu. Rev. Biochem.* **55**, 663-700.

McGraw, T. E., Greenfield, L. and Maxfield, F. R. (1987). Functional expression of the human transferrin receptor cDNA in Chinese hamster ovary cells deficient in endogenous transferrin receptor. *J. Cell Biol.* **105**, 207-214.

McGraw, T. E. and Maxfield, F. R. (1990). Human transferrin receptor internalization is partially dependent upon an aromatic amino acid on the cytoplasmic domain. *Cell Regul.* **1**, 369-377.

McGraw, T. E. and Maxfield, F. R. (1991). Internalization and sorting of macromolecules: endocytosis. In *Targeted Drug Delivery* (ed. R. L. Juliano), pp. 11-41. Springer-Verlag, Berlin.

McGraw, T. E., Dunn, K. W. and Maxfield, F. R. (1993). Isolation of a temperature-sensitive variant Chinese hamster ovary cell line with a morphologically altered endocytic recycling compartment. *J. Cell. Physiol.* **155**, 579-594.

Murphy, R. F. (1991). Maturation models for endosome and lysosome biogenesis. *Trends Cell Biol.* **1**, 77-82.

Pitas, R. E., Innerarity, T. L., Weinstein, J. N. and Mahley, R. W. (1981). Acetoacetylated lipoproteins used to distinguish fibroblasts from macrophages in vitro by fluorescence microscopy. *Arteriosclerosis* **1**, 177-185.

Presley, J. F., Mayor, S., Dunn, K. W., Johnson, L. S., McGraw, T. E. and Maxfield, F. R. (1993). The End2 mutation in CHO cells slows the exit of transferrin receptors from the recycling compartment but bulk membrane recycling is unaffected. *J. Cell Biol.* **122**, 1231-1241.

Salzman, N. H. and Maxfield, F. R. (1988). Intracellular fusion of sequentially formed endocytic compartments. *J. Cell Biol.* **106**, 1083-1091.

Salzman, N. H. and Maxfield, F. R. (1989). Fusion accessibility of endocytic compartments along the recycling and lysosomal endocytic pathways in intact cells. *J. Cell Biol.* **109**, 2097-2104.

Schmid, S. L., Fuchs, R., Male, P. and Mellman, I. (1988). Two distinct subpopulations of endosomes involved in membrane recycling and transport to lysosomes. *Cell* **52**, 73-83.

Sipe, D. M. and Murphy, R. F. (1987). High-resolution kinetics of transferrin acidification in BALB/c 3T3 cells: Exposure to pH 6 followed by temperature-sensitive alkalinization during recycling. *Proc. Nat. Acad. Sci. USA* **84**, 7119-7123.

Snider, M. D. and Rogers, O. C. (1985). Intracellular movement of cell surface receptors after endocytosis: resialylation of asialo-transferrin receptor in human erythroleukemia cells. *J. Cell Biol.* **100**, 826-834.

Stoorvogel, W., Geuze, H. J., Griffith, J. M. and Strous, G. J. (1988). The pathways of endocytosed transferrin and secretory protein are connected in the trans-Golgi reticulum. *J. Cell Biol.* **106**, 1821-1829.

Stoorvogel, W., Strous, G. J., Geuze, H. J., Oorschot, V. and Schwartz, A. L. (1991). Late endosomes derive from early endosomes by maturation. *Cell* **65**, 417-427.

Tooze, J. and Hollinshead, M. (1991). Tubular early endosomal networks in AtT20 and other cells. *J. Cell Biol.* **115**, 635-653.

van Deurs, B., Petersen, O. W., Olsnes, S. and Sandvig, K. (1989). The ways of endocytosis. *Int. Rev. Cytol.* **117**, 131-177.

van Deurs, B., Holm, P. K., Kayser, L., Sandvig, K. and Hansen, S. H. (1993). Multivesicular bodies in HEp-2 cells are maturing endosomes. *Eur. J. Cell Biol.* **61**, 208-224.

Warren, G. (1990). Trawling for receptors. *Nature* **346**, 318-319.

Wells, K. S., Sandison, D. R., Strickler, J. and Webb, W. W. (1990). Quantitative fluorescence imaging with laser scanning confocal microscopy. In *Handbook of Biological Confocal Microscopy* (ed. J. B. Pawley), pp. 27-39. Plenum Publishing Corporation, New York.

Yamashiro, D. J., Tycko, B., Fluss, S. R. and Maxfield, F. R. (1984). Segregation of transferrin to a mildly acidic (pH 6.5) para-Golgi compartment in the recycling pathway. *Cell* **37**, 789-800.

Yamashiro, D. J. and Maxfield, F. R. (1987). Kinetics of endosome acidification in mutant and wild-type Chinese hamster ovary cells. *J. Cell Biol.* **105**, 2713-2721.

(Received 25 February 1994 - Accepted 22 April 1994)